Journal of Power Sources 194 (2009) 818–823

Contents lists available at ScienceDirect

Journal of Power Sources

journal homepage: www.elsevier.com/locate/jpowsour

Short communication

Experimental investigation of current distribution in a direct methanol fuel cell with serpentine flow-fields under various operating conditions

Sang-Min Park[a,b], Sang-Kyung Kim[a,*], Seongyop Lim[a], Doo-Hwan Jung[a], Dong-Hyun Peck[a], Won Hi Hong[b,**]

[a] Fuel Cell Research Center, Korea Institute of Energy Research, 71-2 Jang-dong, Yuseong-gu, Daejeon 305-343, Republic of Korea
[b] Department of Chemical and Biomolecular Engineering (BK21 program), KAIST, 335 Gwahak-ro, Yuseong-gu, Daejeon 305-701, Republic of Korea

ARTICLE INFO

Article history:
Received 6 March 2009
Received in revised form 12 May 2009
Accepted 8 June 2009
Available online 24 June 2009

Keywords:
Direct methanol fuel cell
Current distribution
Serpentine

ABSTRACT

The influences of various operating conditions on the current distribution of a direct methanol fuel cell with flow-fields of serpentine channels are investigated by means of a current-mapping method. The current densities generally deviate more from an even distribution when the cell temperature or flow rate of the cathode reactant is lower, or when the current loaded on the cell or the methanol concentration is higher. In addition, uneven current distributions decrease the cell performance. Relevant mass-transfer phenomena such as water flooding and methanol crossover are discussed. The characteristics of the channel configuration also affect the current density profiles. With a five-line serpentine channel, the current densities are lowered periodically where the flow direction is inverted due to the corner flow effect and the subsequent water accumulation. With a single serpentine channel, on the other hand, the current densities peak periodically where the flow direction is inverted due to enhanced air convection through the gas-diffusion layer.

1. Introduction

The direct methanol fuel cell (DMFC) is a promising power source for portable electronic devices due to its high specific energy, compact design, and simple assembly [1,2]. Sluggish methanol electro-oxidation and methanol crossover are widely recognized as the major technical issues with regard to the further development of DMFCs. Thus, many recent studies have focused on the development and improvement of the catalyst and membrane of DMFCs [3,4].

Another issue in the operation of a DMFC is the management of the mass-transfer phenomena that occur inside this type of fuel cell. Compared with a hydrogen-fed polymer electrolyte fuel cell (PEFC), a DMFC is simple to operate because it directly utilizes liquid methanol as a fuel. On the other hand, the mass-transfer phenomena in a DMFC are more complicated than those in a hydrogen-fed PEFC. During the operation of a DMFC, two-phase flows of a liquid methanol solution and CO_2 gas exist at the anode side, while two-phase flows of air and vapor/liquid water exist at the cathode side [5,6]. Methanol crossover is another important factor that affects mass-transfer in a DMFC [5,7]. Phenomena such as a partial lack of reactants and channel clogging due to water flooding can lead to a non-uniform reactant concentration, which can then cause non-uniform electrochemical reactions and non-uniform utilization of the catalyst layer on the electrode. Continual non-uniformity can give rise to partial ageing or corrosion and thereby reduce the lifetime of the cell [8]. Thus, it is essential to investigate the spatial difference along the surface of the membrane-electrode assembly (MEA) during the operation of these fuel cells.

Several studies have investigated mass-transfer phenomena in fuel cells based on a proton exchange membrane, such as DMFCs and PEFCs. Visualization techniques using a transparent single cell [6,9] or measurement of the current distribution throughout the entire area of the electrode [8,10–14] are useful tools in these endeavours. Measurement of the current distribution in particular can produce a quantitative estimation of spatially different performances along the surface of a MEA during operation. Recently, the mechanism by which mass-transfer phenomena in a single cell affect the current distributions has been reported in relation to PEFCs or DMFCs. Noponen et al. [10], Sun et al. [11] and Ghosh et al. [12] constructed their own devices and analyzed the operational effects of temperature, total current, reactant flow rate and pressure on the current density distributions in hydrogen-fed PEFCs. Saarinen et al. [13] focused on a free-breathing type of DMFC to investigate the effects of an anode reactant. The concentration and flow rate of the methanol were varied for two types of membrane with different levels of methanol permeability. It was that methanol crossover, together with inadequate air convection, caused deviation from an even current distribution. Mench and Wang [14] also

* Corresponding authors. Tel.: +82 42 860 3366; fax: +82 42 860 3739.
** Corresponding authors. Tel.: +82 42 350 3919; fax: +82 420 350 3910.
E-mail addresses: ksk@kier.re.kr (S.-K. Kim), whhong@kaist.ac.kr (W.H. Hong).

0378-7753/$ – see front matter © 2009 Elsevier B.V. All rights reserved.
doi:10.1016/j.jpowsour.2009.06.052

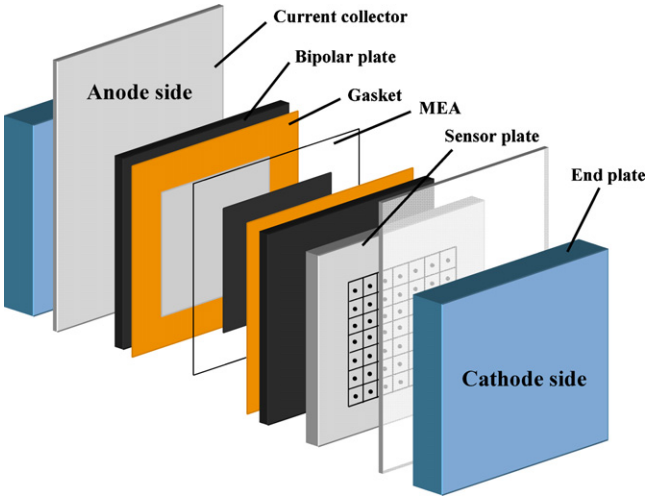

Fig. 1. Schematic of single cell for measurement of current density distribution.

studied the current distribution in a DMFC to analyze the mass-transfer behaviour that occurs at the cathode side. Cathode flooding was predicted from the measurement of the current distribution and relevant equations, although the effects of other factors such as the methanol feeding conditions and the operating temperature were not investigated. Ay et al. [8] examined the effects of the operating parameters on the current density of DMFCs. The channel configuration was not specified and there were only nine segments, which was a relatively low number given the active area of the cell.

The present study uses a current-mapping method to investigate the effects of the operating conditions on the current distribution in a DMFC in an effort to obtain useful information regarding the mass transport–related phenomena that occur during the operation of the system. The reactant flow rate, the reactant concentration, the cell temperature and the load current were all varied. A flow-field with a serpentine channel configuration was used on both electrodes as it outperforms the parallel, interdigitated, or grid configurations if the required pressure drop is disregarded [6,15–17]. Accordingly, the effects of this flow-field configuration on the current distribution profile were also evaluated.

2. Experimental

2.1. Device for current distribution measurement

Current Scan Lin (S++®) was used in this study as the current-mapping device. As shown schematically in Fig. 1, the MEA was sandwiched between two bipolar plates, and a sensor plate was placed between the bipolar plate and the end-plate on the cathode side. The sensor plate was segmented into 49 positions, as shown in Fig. 2; But, the gas-diffusion layer (GDL) at the cathode side was not segmented due to the rational accuracy of the current density measurement system [10,14]. The current density was measured at each of the 49 segments. The segmentation was numbered from the inlet to the outlet on the basis of the cathode flow. On the anode side, the inlet was located at segment 42 and the outlet was located at segment 7, and the flow directions were opposite to those of the cathode at every line of the channel. As depicted in Fig. 2, when five-line serpentine flow-fields were used, each segment of the sensor plate corresponded to the current collected from an area of 0.51 cm^2 with 5 channels and 5 ribs.

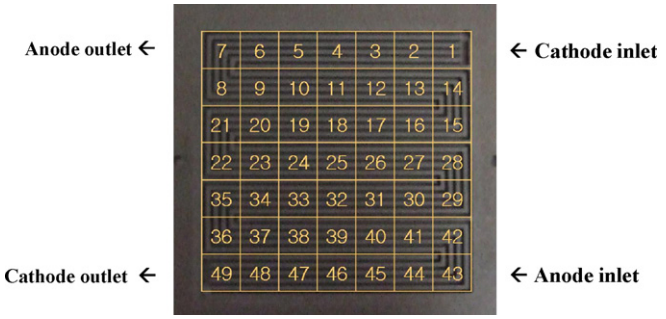

Fig. 2. Segment positions of measurement cell along channel.

2.2. Preparation of MEA

The catalysts were PtRu black (HiSpec 6000™, Johnson Matthey) for the anode and Pt black (HiSpec 1000™, Johnson Matthey) for the cathode. To prepare the catalyst slurry, 10 wt% of Nafion (5 wt% Nafion solution) was mixed with PtRu black and the mixed solution was diluted with an excessive amount of isopropanol for dispersion with an ultrasonic processor. For the cathode, 7 wt% of Nafion (5 wt% Nafion solution) was added to Pt black, and the following procedure was the same as that for the anode. The gas-diffusion layer for the anode, TGP-H-060 (Toray), was pretreated with a 5 wt% Teflon solution, and Sigracet 25BC (SGL) was used as the cathode. The catalyst slurries were brushed on to the electrode at a loading of 4 mg cm^{-2} Pt for the anode side and 5 mg cm^{-2} Pt for the cathode side. The membrane electrode assembly was prepared by placing a Nafion 115 (Du Pont) membrane between the two electrodes and hot-pressing these three components at 150 °C for 1 min under a pressure of 100 kgf cm^{-2}. The active area of the MEA was 25 cm^2 (5 cm × 5 cm).

2.3. Measurement of current distribution under different operating conditions

To investigate the influence of the operating conditions on the current density of the DMFC, the operating parameters of the total current, the cell temperature, the reactant flow rate, the reactant concentration and the configuration of the flow-field were varied. For the measurements, the cell was operated in the galvanostatic mode, and the stoichiometric factors were calculated on the assumption that the fed reactants were all consumed by the following chemical reactions:

Anode:

$$CH_3OH + H_2O \rightarrow CO_2 + 6H^+ + 6e^- \quad (1)$$

Cathode:(2) $\frac{3}{2}O_2 + 6H^+ + 6e^- \rightarrow 3H_2O$

Overall: (3) $CH_3OH + \frac{3}{2}O_2 \rightarrow CO_2 + 2H_2O$

Unless otherwise specified, the basic operating conditions were as follows: a total current of 2 A or 5 A loaded on a single cell, stoichiometric factors (λ) of 20 for the anode and 13 for the cathode, a methanol concentration of 2 M, a cell temperature of 60 °C, and a five-line serpentine flow channel. The channel had a channel depth of 0.7 mm, a channel width of 0.7 mm, and a rib width of 0.7 mm. The current was loaded on to a single cell for 3 min while the cell voltage was measured simultaneously. The current distributions and the cell voltages presented in the following section represent the data obtained when 2 min have passed since the current was loaded on to the single cell.

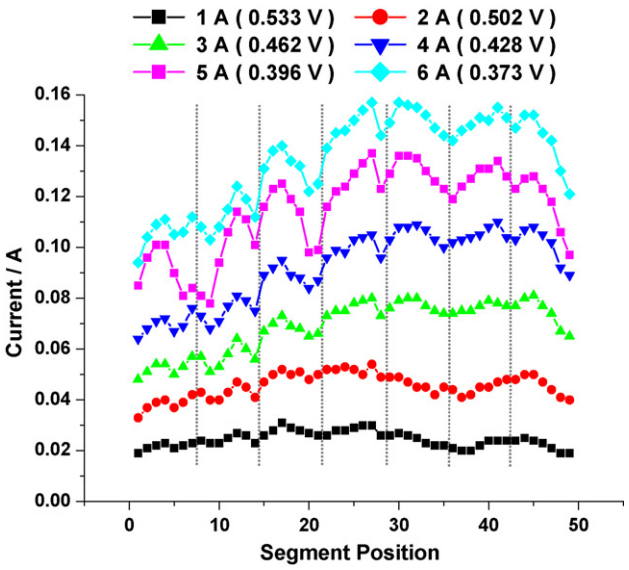

Fig. 3. Current distributions for different currents loaded on a single cell.

3. Results and discussion

3.1. Effect of current loaded on to cell

First, the total current loaded on to the single cell was varied from 1 A to 6 A. The current distribution profiles for the six current levels and the corresponding cell voltages are shown in Fig. 3. As expected, the cell voltage decreases as the total current increases. Overall, the current densities appear to be homogeneously distributed along the channel because the reactants are fed at high flow rates (λ = 20 for the anode side and λ = 13 for the cathode side). The current is the most homogeneously distributed at the lowest total current (1 A), and the degree of deviation from homogeneity increases as the total current loaded increases; the current near the cathode outlet (in other words, near the anode inlet) becomes higher than the current near the cathode inlet. This phenomenon is discussed below in Section 3.3.

It is also found that the current density appears lower periodically at positions where the flow direction is inverted (dotted line in Fig. 3), namely, in the U-bend region [18]. These regions are near segments 14, 21 and 28 (and continuing in steps of seven) with the exception of segment 7. In addition, the periodical drops are more clearly observable when the total current is higher. This phenomenon is ascribed to the configuration of the five-line serpentine flow-field. The positions where the flow direction is inverted are regions of low velocity due to the corner flow effect [18,19]. Thus, a decrease in the velocity leads to a lack of reactant, and retards sweeping out of the water or vapour produced near this region. This can lead to an intermittent decrease in the current density profiles. This region is discussed further and compared with another flow-field in Section 3.5.

For further investigation of the effects of the operating parameters, two currents of 2 A and 5 A were selected as they correspond to cell voltages of approximately 0.5 V and 0.4 V.

3.2. Effect of temperature

It is well known that the operating temperature is an important determinant of DMFC performance and that a temperature elevated above ambient or near ambient is advantageous due to the lowered activation energy [3]. In this study, the temperature of the cell was varied to investigate its effect on the current distribution for two

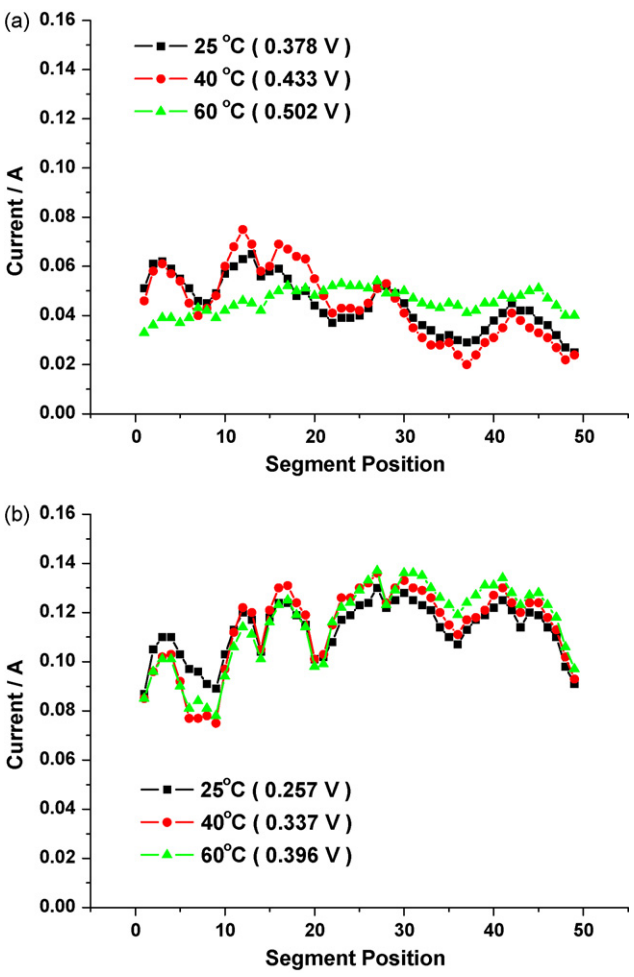

Fig. 4. Current distributions at different cell temperatures with a loaded current of (a) 2 A and (b) 5 A.

different current loads of 2 A and 5 A. The resulting current densities are relatively homogeneously distributed along the channel at 60 °C. The current density is higher near the cathode inlet than near the cathode outlet at temperatures of the ambient temperature (25 °C) and 40 °C. This behaviour indicates that water flooding occurs near the cathode outlet. At lower temperatures, the water produced at the cathode side cannot easily be vaporized. On the other hand, there are no noticeable differences in the current distribution at the different temperatures with the higher current of 5 A, see Fig. 4(b). The flow rate for both sides should be sufficiently high to satisfy the stoichiometric factors (λ) of 20 13 for the anode and the cathode, respectively. The blown effect of the high flow rate may therefore deter the accumulation of water near the cathode outlet [11]. The cell voltage decreases with decrease in cell temperature for both 2 A and 5 A, as shown in Fig. 4. This is because the cell performance is mainly affected by the cell temperature [1].

3.3. Effects of flow rates

The current distributions at different flow rates on the cathode side when a current of 2 A is imposed are presented in Fig. 5(a). When the flow rate (λ) at the cathode is reduced from 13 to 3, the cell voltage drops from 0.5 V to 0.4 V, and the difference in current between the cathode inlet and the cathode outlet increased. For a low flow rate at the cathode, the water flooding caused by the lack of air and the reduced oxygen mass fraction towards the cathode outlet lead to lower current densities at the cathode outlet and a

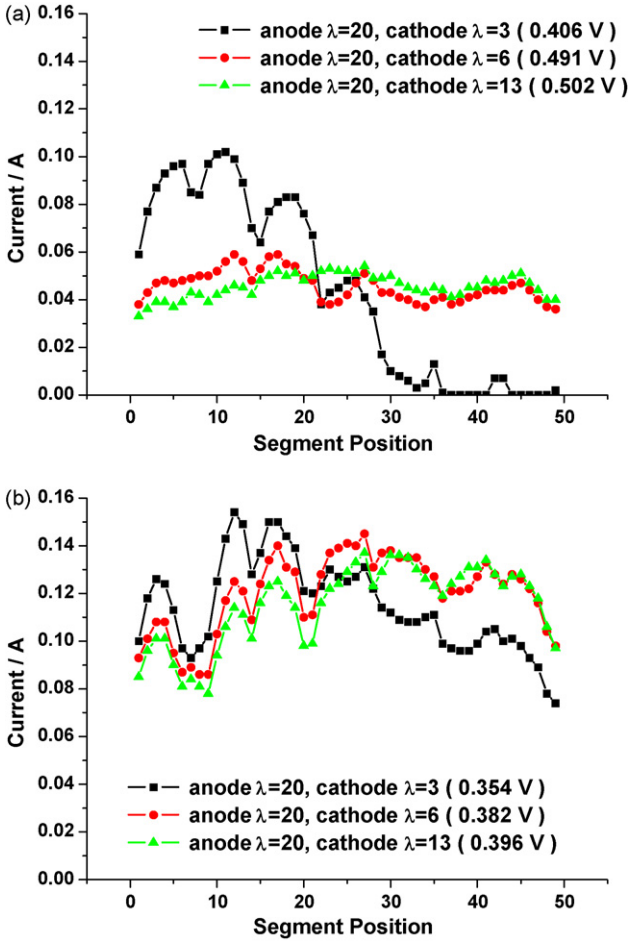

Fig. 5. Current distributions at different air flow rates with loaded current of (a) 2 A and (b) 5A.

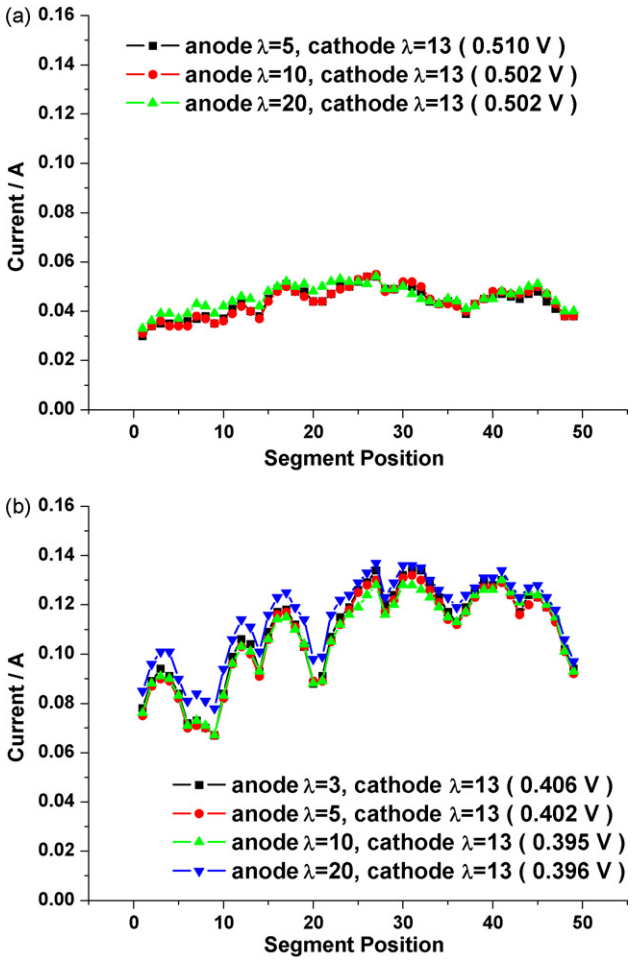

Fig. 6. Current distributions at different methanol flow rates with loaded current of (a) 2 A and (b) 5 A.

decreased cell voltage [14,15]. At a higher current (5 A), however, the inhomogeneity of the current distribution is less apparent as shown in Fig. 5(b). Furthermore, the drop in the cell voltage as the cathode flow rate decreases is smaller than that at a current of 2 A, as shown in the legend of Fig. 5. This phenomenon occurs because, as discussed in Section 3.2, the flow rates required to satisfy the stoichiometric factors of 6 or 3 at this current (5 A) remain high enough to prevent water flooding; moreover, near the cathode outlet, the oxygen mass fraction is sufficient for the reduction reaction [15].

The current distributions at different flow rates of the methanol solution are reported in Fig. 6. The reduced flow rate at the anode does not affect the current density distribution; but, as presented in the legend of Fig. 6, there are slight decreases in the cell voltage when the flow rate is increased. The current density is distributed relatively homogeneously, regardless of the anode flow rate, especially at the low current of 2 A. A slight decrease in the cell voltage at a higher flow rate suggests an increase in crossover through the Nafion membrane [13].

The current densities at 5 A, given in Fig. 6 (b), appear to increase slightly down to the cathode outlet from approximately 0.07 A to 0.14 A and then decrease again to 0.07 A at the cathode outlet. In terms of the anode flow, the current densities near the anode inlet are higher than those near the anode outlet. This phenomenon correlates with methanol consumption, the evolution of CO_2 gases, and partial drying of the membrane near the cathode inlet [14]. The methanol concentration becomes lower towards the anode outlet because methanol is used steadily along the flow channel. The void fraction generated by the CO_2 gases produced from the anode reaction becomes higher along the anode channel [5,6,20,21]. Both the decreased methanol concentration and the increased void fraction toward the anode outlet are likely causes for the gradual decrease in current density toward the anode outlet. In addition, local drying of the membrane near the cathode inlet contributes to the reduction in the current density in this region [14].

3.4. Effects of methanol concentration

Current densities for different methanol concentrations were examined. The current distribution at different air flow rates and methanol concentrations of 1 M and 2 M are given in Fig. 7. The air stoichiometry (λ) was varied from 2 to 13, whereas the stoichiometry values at the anode side were set to 10 for all cases. As discussed earlier, the reduced air flow rate lowers the current densities at the cathode outlet when 2 M methanol is used. With 1 M methanol, however, the current density is generally distributed homogeneously throughout the MEA regardless of the air flow rate. As seen in the legend of Fig. 7, the drop in the cell voltage, caused by a decrease in the air flow rate, is less with 1 M methanol than with 2 M methanol. These results show that the current distributions are affected not only by the flow rates at the cathode but by the methanol concentration fed to the anode side, even when the flow rates at the cathode side are the only variable. It is widely known that methanol passing through the membrane is oxidized at the cathode and thereby diminishes the electrode potential [4,13]. In this study, the decrease in the current density toward the cath-

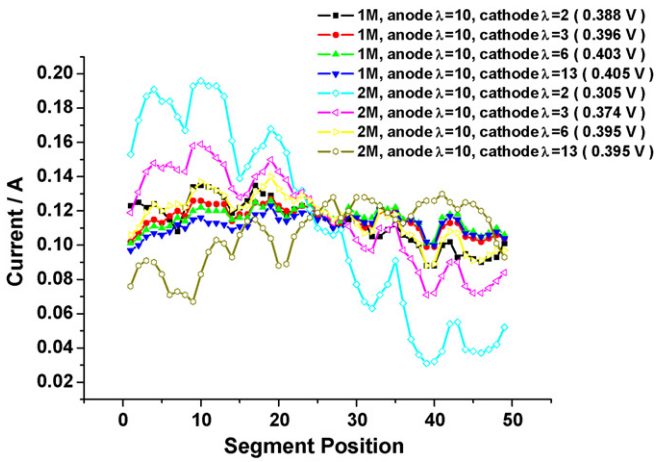

Fig. 7. Current distributions at different methanol concentrations and different air flow rates, with loaded current of 5 A.

ode outlet that accompanies a decrease in the air flow rate occurs more readily at a methanol concentration of 2 M. This behaviour indicates that the increased methanol crossover at a higher concentration of 2 M causes mixed-potential effect [7], whereas the effects of the methanol crossover is rarely observed at the relatively low concentration of 1 M.

The same comparisons were made for the anode side, as presented in Fig. 8. The Data reveal that a slight decrease in current density toward the anode outlet, as reported in Section 3.3, is not commonly observed at a low concentration of 1 M, regardless of the anode flow rate. The methanol concentration decreases along the methanol path as a result of its electrochemical consumption [5], and the higher methanol concentration from the anode inlet increases the methanol crossover [7]. Near the anode outlet, a greater amount of methanol is able to pass to the cathode side when 2 M of methanol is used, as the methanol concentration is still higher than when 1 M of methanol is used in this region. Given that all the experiments in this investigation were performed in a galvanostatic mode, the same amount of current was loaded in both cases. Accordingly, the lowered current distribution near the anode outlet requires some compensation to be made near the anode inlet. Thus, the current densities are higher near the anode inlet when 2 M of methanol is used.

A comparison of the results given in Figs. 7 and 8 shows that the current distribution appears to be affected more by the cathode flow rate than by the anode flow rate when 2 M of methanol is used. Interestingly, this effect provides indirect evidence of methanol crossover, and confirms that the oxidation of crossed-over methanol is easy when the air flow rate is high.

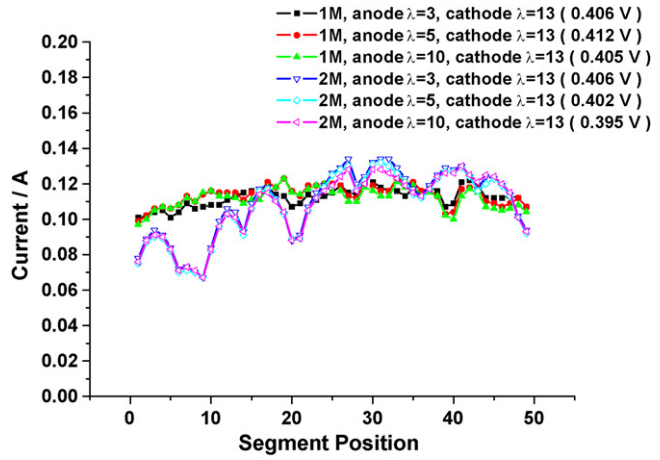

Fig. 8. Current distributions at different methanol concentrations and different methanol flow rates, with loaded current of 5 A.

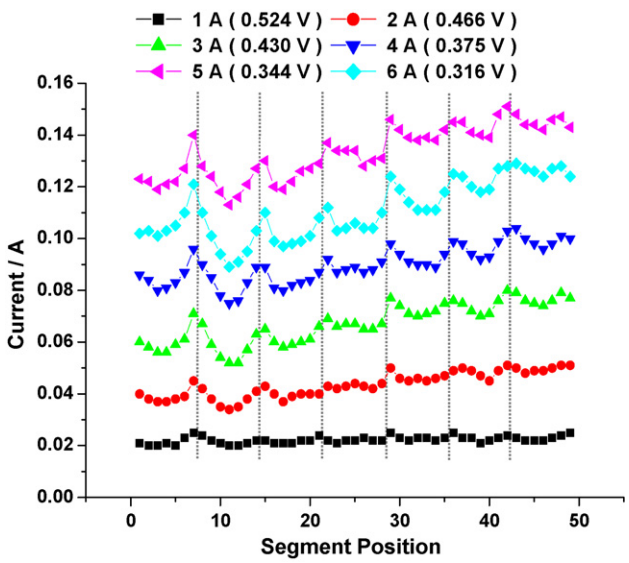

Fig. 9. Current distributions at different currents loaded on a single cell with one-line serpentine flow-field on cathode side.

3.5. *Effect of flow-field configuration*

The data in Fig. 3 showed that the current densities are lowered periodically at the position where the flow direction is inverted with the five-line serpentine channel due to the low velocity and the accumulation of water. In a more detailed investigation of the influence of the flow-field configuration on current density distribution and cell performance, the flow-field at the cathode side was changed to a single (one-line) serpentine channel while that at the anode side was left unchanged. The current density distribution with this channel configuration for currents ranging from 1 A to 6 A is given in Fig. 9. In contrast to the results shown in Fig. 3, the current density appears to peak periodically at the position where the flow direction is inverted (dotted line) when the single serpentine channel is used. This feature is more noticeable at higher currents.

As discussed in Section 3.1, the configuration of the U-bend contributes to the periodical change of current density. The differences between the two flow-fields in the local currents near the U-bend region can be explained directly, as follows. As shown in Fig. 2, each segment covers an area of 0.51 mm^2 (7.1 mm × 7.1 mm), which corresponds to five-line of the channel and five-line of the rib. Fig. 10(a) shows segment A and segment B, which correspond to the middle and the U-bend region of a row of segments, respectively. At segment A, the flow direction of the air is identical for all five channels, as described in Fig. 10(a), and the flow is affected by the pressure difference, which is determined by the air flow rate and the channel distance from the inlet [22]. At segment B, on the other hand, the air velocity becomes lower where the air meets the L-shaped channel due to corner flow effects [18,19]. Consequently, the water that forms as a result of the oxygen reduction cannot be removed easily from this region, and the resultant flooding reduces the electrochemically active area and lowers the current density.

For a single serpentine channel, however, the characteristics of the flow at the U-bend region differ from those of the five-line serpentine channel despite the fact that both of these channels are based on the serpentine configuration. In Fig. 10(b), the air flow direction is inverted at every line of the channel; this condition sat-

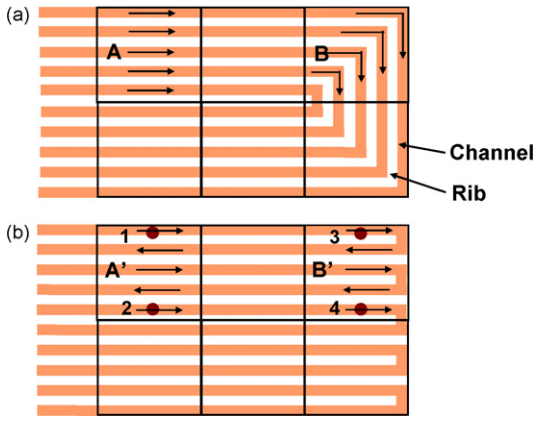

Fig. 10. Fluid flow for two types of flow-field: (a) five-line serpentine and (b) single serpentine.

isfies the flow through the porous GDL under the ribs, known as under-rib convection [22]. The pressure difference between points 1 and 2 in Fig. 10(b) at segment A′, $\Delta P_{1,2}$, corresponds to the pressure difference across the four ribs between point 1 and point 2. This can be approximated using the Hagen–Poiseuille equation, as follows [22,23]:

$$\Delta P_{1,2} = \frac{128\mu Q}{\pi D_{\text{eff}}^4} L_{\text{r}} \times 4 \quad (4)$$

where D_{eff}: effective dynamic diameter of the fluid flow, μ: viscosity, Q: mass flow rate of the fluid, L_{r}: rib length

For segment B′, the pressure difference between points 3 and 4 for under-rib convection is also satisfied because the number of ribs and the flow direction match the conditions of segment A′. In the U-bend regions at the end of segment B′, however, the reactant has difficulty flowing in along the channel due to the corner flow effect. Instead, the reactant flows into the GDL and catalyst layer [22,24]; thus, under-rib convection can arise more readily in this region than at segment A′. The enhanced convection of the cathode reactant at this segment may enhance the electrochemical reaction at the reaction area and thereby generate high local current densities.

4. Conclusions

The influence of different operating parameters on the current distribution in a DMFC has been examined by means of a current-mapping method. A flow-field with a serpentine channel configuration is used for both electrodes due to its superior performance relative to other configurations. From the observed unevenness of the current distribution, the following useful information regarding the relevant mass-transfer phenomena has been obtained:

(i) The inhomogeneity of current distribution is provoked by a low cell temperature, a low cathode flow rate, a high load current and a high methanol concentration. In most cases apart from the total current loaded, inhomogeneity is accompanied by a decrease in cell voltage. This suggests that uneven current distribution can decrease cell performance.

(ii) Even when the flow rate at the cathode is relatively low, the current is evenly distributed along the surface of the MEA when the methanol concentration is low. This observation indicates that the mixed-potential effect from methanol crossover seldom occurs at a low methanol concentration.

(iii) The design of the channel configuration also affects the current density profile. With a five-line serpentine channel at the cathode, the current density is lowered periodically where the flow direction is inverted; this behaviour is due to the low air velocity caused by the corner flow effect and the subsequent water accumulation. With a single serpentine channel at the cathode, however, the current densities peak periodically where the flow direction is inverted as a result of the enhanced air convection through the GDL.

Acknowledgement

This research was supported by the New & Renewable Energy Project of the Ministry of Knowledge Economy, Korea.

References

[1] J. Larminie, A. Dicks, Fuel Cell System Explained, second ed., Wiley, Chichester, 2003.
[2] B.-D. Lee, D.-H. Jung, Y.-H. Ko, J. Power Sources 131 (2004) 207–212.
[3] H. Liu, C. Song, L. Zhang, J. Zhang, H. Wang, D.P. Wilkinson, J. Power Sources 155 (2006) 95–110.
[4] Y.J. Kim, W.C. Choi, S.I. Woo, W.H. Hong, Electrochim. Acta 49 (2004) 3227–3234.
[5] Z.H. Wang, C.Y. Wang, J. Electrochem. Soc. 150 (2003) A508–A519.
[6] H. Yang, T.S. Zhao, Q. Ye, J. Power Sources 139 (2005) 79–90.
[7] S. Eccarius, B.L. Garcia, C. Hebling, J.W. Weidner, J. Power Sources 179 (2008) 723–733.
[8] F. Ay, A. Ata, H. Dohle, T. Sener, H. Gorgun, J. Power Sources 167 (2007) 391–397.
[9] F.Y. Jang, X.G. Yang, C.Y. Wang, J. Electrochem. Soc. 153 (2006) A225–A232.
[10] M. Noponen, T. Mennola, M. Mikkola, T. Hottinen, P. Lund, J. Power Sources 106 (2002) 304–312.
[11] H. Sun, G. Zhang, L.-J. Guo, H. Liu, J. Power Sources 158 (2006) 326–332.
[12] P.C. Ghosh, T. Wuster, H. Dohle, N. Kimiaie, J. Mergel, D. Stolten, J. Power Sources 154 (2006) 184–191.
[13] V. Saarinen, O. Himanen, T. Kallio, G. Sundholm, K. Kontturi, J. Power Sources 163 (2007) 768–776.
[14] M. Mench, C.Y. Wang, J. Electrochem. Soc. 150 (2003) A79–A85.
[15] G.-B. Jung, A. Su, C.-H. Tu, Y.-T. Lin, F.-B. Weng, S.-H. Chan, J. Power Sources 171 (2007) 212–217.
[16] M.S. Hyun, S.-K. Kim, D. Jung, B. Lee, D. Peck, T. Kim, Y. Shul, J. Power Sources 157 (2006) 875–885.
[17] X. Li, I. Sabir, Int. J. Hydrogen Energy 30 (2005) 359–371.
[18] K.B. Prasad, S. Jayanti, J. Power Sources 180 (2008) 227–231.
[19] D. Spernjak, A.K. Prasad, S.G. Advani, J. Power Sources 170 (2007) 334–344.
[20] V.A. Danilov, J. Kim, I. Moon, H. Chang, J. Power Sources 162 (2006) 992–1002.
[21] D.U. Sauer, T. Sanders, B. Fricke, T. Baumhofer, K. Wippermann, A.A. Kulikovsky, H. Schmitz, J. Mergel, J. Power Sources 176 (2008) 477–483.
[22] C. Xu, T.S. Zhao, Electrochem. Commun. 9 (2007) 497–503.
[23] I. Garnet, Fluid Mechanics, fourth ed., Prentice Hall, Englewood Cliffs, 1996.
[24] X.-D. Wang, Y.-Y. Duan, W.-M. Yan, X.-F. Peng, J. Power Sources 175 (2008) 397–407.